JPE 14-6-19

http://dx.doi.org/10.6113/JPE.2014.14.6.1254
ISSN(Print): 1598-2092 / ISSN(Online): 2093-4718

Study on the Temperature Drift Adaptive Compensation Algorithm of a Magneto-Electric Encoder Based on a Simple Neuron

Lei Wang*, Shuang-hui Hao*, Bao-yu Song*, and Ming-hui Hao†

*†School of Mechanical Engineering, Harbin Institute of Technology, Harbin, China

Abstract

Magneto-electric encoders have been widely used in industry and military applications because of their good shock resistance, small volume, and convenient data processing. However, the characteristics of a magneto-electric encoder's signal generator and hall sensor changes minimally with temperature variation. These changes cause an angle drift. The main purpose of this study is to construct the compensation system of a neural network and constantly update weight coefficients of temperature correction by finite iteration calculation so that the angle value modified can approach the angle value at the target temperature. This approach is used in adaptive correction of the angle value.

Key words: Magneto-electric encoder, Neurons temperature compensation algorithm, Temperature drift, Zero-point drift

I. INTRODUCTION

Encoders that can translate rotary motion into electrical signals represent the most popular angular transducer. It is widely used in several applications, such as mechanical engineering, robotics, astronomical applications, precision optics, and high-performance controllers. It also plays an important role in modern industry, especially in motor control. Motor control relies on the accuracy and achievable resolution from the encoder [1], [2].

Currently, high-accuracy encoders can be divided into two categories, namely, magnetic and optical encoders. An optical encoder is an opto-mechanical-electronic device that transforms light distribution into two sinusoidal electrical signals that are used to determine the relative position between a scanning head and a scale (linear or angular) [3]. This encoder type is small, lightweight, and characterized by high response frequencies and resolutions. Although optical encoders are widely used in industrial applications, they have some significant disadvantages. First, they are made of easily breakable materials and are costly. They are also unsuitable for several special situations because of their frangibility and bad mounting environment; they also accumulate reading errors and loss of position caused by power interruptions [4], [6]. Magnetic encoders are based on the principles of reading and writing to magnetic media. Unlike optical encoders, magnetic encoders are characterized by their strong anti-interference ability and are unaffected by dusty and misty conditions. Given that the code disk can be recorded and erased repeatedly, magnetic rotary encoders are suited for small-lot production.

However, magnetic encoders also have some drawbacks. A typical magnetic encoder is described as follows: Under different temperatures, the features of the signal generating components and hall sensors of the magnetic encoder change slightly. As a result, angle temperature drift occurs. Several methods that attempt to solve the abovementioned problems were presented in [7], [8], and traditional solutions have been proposed. The compensation method in hardware is presented in [7]. Four sensor elements are connected in each unit of the MAGFET array such that the signal currents of the magnetic field are added and offset currents caused by the piezo-resistive effect are canceled out. A compensation technique that uses the successive approximation algorithm is presented in [8]. A novel method for continuous time calibration of hall sensors has been proposed. It can eliminate all drift sources, including temperature drift. Among the

Manuscript received Apr. 25, 2014; accepted Jul. 16, 2014
Recommended for publication by Associate Editor Kwang-Woon Lee.
†Corresponding Author: hao_minghui@163.com
Tel: +864-716-92, Fax: +864-021-49, Harbin Institute of Technology
*School of Mechanical Engineering, Harbin Institute of Technology, China

© 2014 KIPE

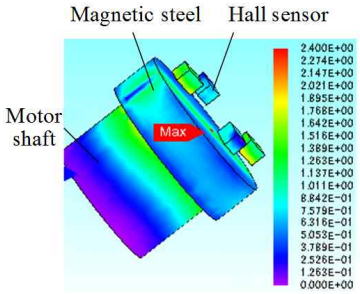

Fig. 1. Magneto-electric encoder structure.

intelligent compensation methods, the artificial neural network compensation method has some advantages, such as less demand for the sample number [9], having a simple algorithm, and ability of arbitrary function approximation [10]. A novel design model based on slant multi-phase filter theory is presented in [11]. The nth harmonic voltage [n = 2nd, 3rd, and 4th... (V)] can be decreased easily. Magnetic encoders with a sinusoidal output voltage waveform have been developed. The sinusoidal output waveform can be easily improved, and the angle drift with temperature can be decreased. A novel magnetic encoder has also been presented in [12], which utilizes an iterative algorithm to suppress the angle drift when temperature changes. The implementation aspects of cyclic and tracking displacement converters based on a single-chip integrated microcircuit of a sine-cosine magnetic encoder have been proposed in [13].

The reason for the angle drift in magnetic encoders when during temperature change is analyzed in Section III. We construct a compensation system of temperature drift in Section III to solve the problem above. A temperature compensation-modified algorithm based on neurons is presented. The temperature weight coefficient is updated constantly through finite iterative computation, which causes the drifting angle at low temperature to approach the target angle at normal temperature automatically. The gradient method used in this paper also implements the fastest convergence of the neutron iterative calculation. Thus, the angle value of the magnetic encoder can be calibrated at different temperatures at the same mechanical position. Experiments are performed in Section IV to verify the efficiency of this method. Finally, conclusions and several remarks are discussed in Section V.

II. Structure of a Magneto-Electric Encoder and Principal of Angle Calculate

Fig. 1 shows the structure of the magneto-electric encoder. It has four halls divided by 90° in a circle.

Under the action of single pole magnetic steel, four signals with a phase difference of 90° were produced on the hall sensor and the signal value centered at approximately 2.5 V [Fig. 2(a)]. The hall signals A+, A-, and B+, B- are subtracted

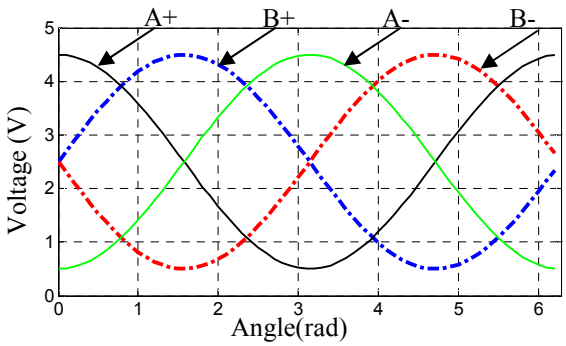

(a)

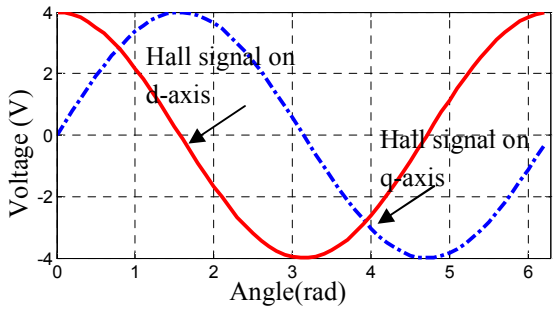

(b)

Fig. 2. Original hall signals of the encoder and signal on the d- and q-axes. (a) Original hall signals. (b) Hall signal on the d- and q-axes.

as shown in Formulas (1) and (2), then the hall value of the d- and q-axes is obtained, as shown in Fig. 2(b).

$$q\_hall = A_+ - A_- \tag{1}$$

$$d\_hall = B_+ - B_- \tag{2}$$

Arctangent Formula (3) is used to calculate the angle of the magneto-electric encoder.

$$\theta = arc\tan(\frac{q\_hall}{d\_hall}) \tag{3}$$

III. Analysis of the Characteristics of the Magneto-Electric Encoder's Temperature Drift and Compensation Algorithm Based on Neuron Theory

A. Analysis of the Angle Drift of a Magneto-electric Encoder

The calculation of a magneto-electric encoder's angle is based on the analog value obtained by hall sensors. The drift of the analog value has two types: temperature drift and zero-point drift. We set variable b_i as the error value of the zero-point drift. The temperature drift amplifies or lowers the ratio of the hall signal amplitude. We set this value to k_i. The value of d_d and q_d after temperature change should then be as follows:

$$d_d = d_c \times k_1 + b_1 \tag{4}$$

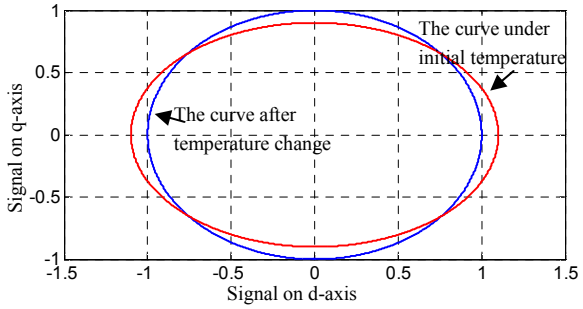

(a) $k_1 = 1.1$, $k_2 = 0.9$, $b_1 = b_2 = 0$.

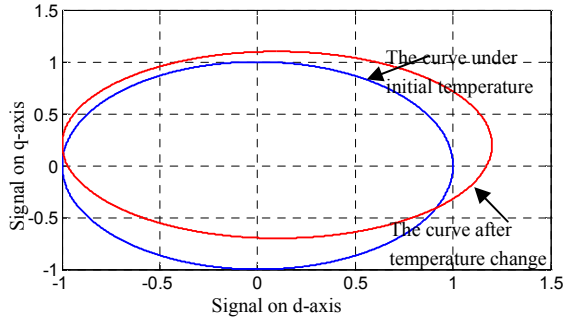

(b) $k_1 = 1.1$, $k_2 = 0.9$, $b_1 = 0.1$, $b_2 = 0.2$.

Fig. 3. Zero-point drift and temperature drift on the influence of the original signal.

$$q_d = q_c \times k_2 + b_2 \tag{5}$$

where d_d is the AD value of the hall on the d-axis after temperature change, q_d is the AD value of the hall on the q-axis after temperature change, d_c is the AD value of the hall on the d-axis under the initial temperature, and q_c is the AD value of the hall on the q-axis under the initial temperature.

Fig. 3 shows the zero-point drift and temperature drift effect on the angle drift.

The picture above clearly shows that if we want to correct the angular deviation because of temperature change, we need to modify the hall value of the d- and q-axes to the value under the initial temperature.

B. Temperature Compensation Algorithm based on a Simple Neuron

Fig. 4 shows the deviation of the hall signal curve caused by temperature change. The previous analysis clearly shows a group of ideal values (i.e., k_1, k_2, b_1, and b_2) that can completely modify the curve deviation.

$$h(\vec{x}) = (h(x_1), h(x_2) \ldots h(x_n)) \tag{6}$$

Suppose the following approximating function:

$$h(\vec{\gamma}, \vec{\omega}) = \sum_{i=1}^{n} B_i(\gamma) \times \omega_i \tag{7}$$

$B_i(\gamma)$ is the benchmark function.

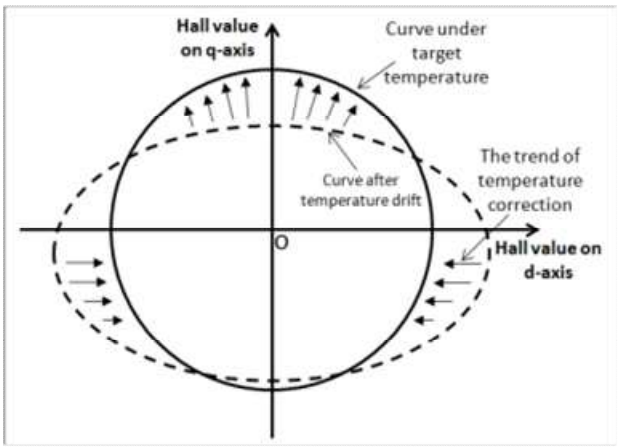

Fig. 4. Diagram of the temperature drift correction process.

Suppose the following target function:

ω_i is the modification weight coefficient. Thus, the error measuring function should be as follows:

$$V_{(x,\gamma,\omega)} = (h(\vec{x}) - \sum_{i=1}^{n} B_i(\gamma) \times \omega_i) \tag{8}$$

This study directly uses the hall value on the d-axis d_d and q-axis q_d, whose changes are caused by the temperature drift as benchmark function $B_i(\gamma)$. Thus,

$$B(\gamma) = B(d_d, q_d) \tag{9}$$

where d_d is the AD value of the hall on the d-axis after temperature drift, and q_d is the AD value of the hall on the q-axis after temperature drift. ω_1, ω_2, ω_3, and ω_4 are taken as the weight coefficients, and the compensation function is built as the neural network output. Thus,

$$d_f = \omega_1 d_d + \omega_2 \tag{10}$$

$$q_f = \omega_3 q_d + \omega_4 \tag{11}$$

where d_f is the value of the d-axis after modification, q_f is the value of the q-axis after modification, ω_1, ω_3 is the weight coefficient of the hall temperature drift, and ω_2, ω_4 is the weight coefficient of hall zero point drift. A structure diagram of the temperature compensation based on a neural network is shown in Fig. 5. The iterative calculation of a neuron algorithm is used to determine the best weight coefficient ω_1, ω_2, ω_3, and ω_4. These four weight coefficients are used to modify d_d and q_d after the temperature drift and cause d_f and q_f to approach d_c and q_c under the target temperature. The approximating function $h(d_d, q_d, \vec{\omega})$ is intended to approach the target function $h(d_c, q_c)$.

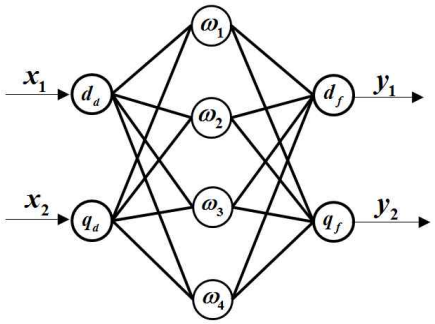

Fig. 5. BP neural network temperature compensation structure.

The error measuring function is constructed as follows:

$$\begin{aligned} & V(X) \\ &= \frac{1}{2}\sum_{i=1}^{n}(h(\vec{x})-\sum_{i=1}^{n}B_i(\gamma)\times\omega_i)^2 \\ &= \frac{1}{2}\sum_{i=1}^{n}(d_f^2+q_f^2-d_c^2-q_c^2)^2 \\ &= \frac{1}{2}\sum_{i=1}^{n}((\omega_1 d_d+\omega_2)^2+(\omega_3 q_d+\omega_4)^2-d_c^2-q_c^2)^2 \end{aligned} \tag{12}$$

The error measuring function in this study is a non-negative value. The value of the error measuring function should decrease by continuously regulating ω_1 , ω_2 , ω_3 , and ω_4 during the iterative calculation process to cause d_f and q_f to approach d_c and q_c under the target temperature. The steep descent direction of the error measuring function $V(X)$ to ω_1 , ω_2 , ω_3 , and ω_4 needs to be determined first to make the error measuring function decrease rapidly to ensure that the angle compensation can be completed in the least iteration times. Thus,

$$\frac{\partial V}{\partial \omega_1}=2\sum_{i=1}^{n}(d_{fi}^2+q_{fi}^2-d_{ci}^2-q_{ci}^2)d_{fi}d_{di} \tag{13}$$

$$\frac{\partial V}{\partial \omega_2}=2\sum_{i=1}^{n}(d_{fi}^2+q_{fi}^2-d_{ci}^2-q_{ci}^2)d_{fi} \tag{14}$$

$$\frac{\partial V}{\partial \omega_3}=2\sum_{i=1}^{n}(d_{fi}^2+q_{fi}^2-d_{ci}^2-q_{ci}^2)q_{fi}q_{di} \tag{15}$$

$$\frac{\partial V}{\partial \omega_4}=2\sum_{i=1}^{n}(d_{fi}^2+q_{fi}^2-d_{ci}^2-q_{ci}^2)q_{fi} \tag{16}$$

From the characteristic of the error measuring function, the function is non-negative to ensure that the function can approach zero fastest in the negative gradient direction and quickly implement the result of d_f and q_f approaching d_c and q_c. Let T be the iteration step. Thus,

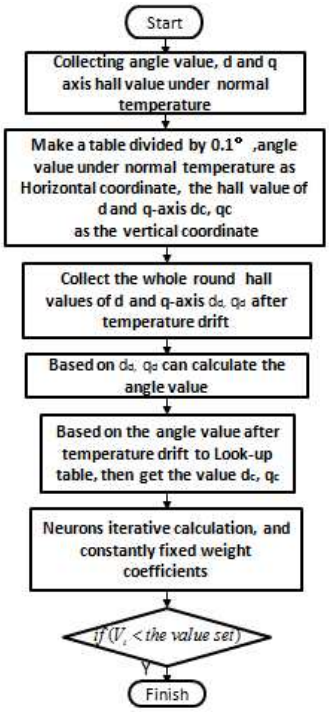

Fig. 6. Flowchart of the temperature correction algorithm.

TABLE I
HALL VALUES OF D-Q AXIS

0°	d_1 Hall value	q_1 Hall value
0.1°	d_2 Hall value	q_2 Hall value
.	.	.
.	.	.
359.9°	d_{3600} Hall value	q_{3600} Hall value

$$\omega_{1(k+1)}=\omega_{1(k)}-\frac{\partial V}{\partial \omega_1}T \tag{17}$$

$$\omega_{2(k+1)}=\omega_{2(k)}-\frac{\partial V}{\partial \omega_2}T \tag{18}$$

$$\omega_{3(k+1)}=\omega_{3(k)}-\frac{\partial V}{\partial \omega_3}T \tag{19}$$

$$\omega_{4(k+1)}=\omega_{4(k)}-\frac{\partial V}{\partial \omega_4}T \tag{20}$$

The neuron modification process is shown in Fig. 6. The data acquisition system is used to collect the angle value θ_c of the whole round under +20 °C as the initial angle value, hall value on d-axis d_c, and hall value on q-axis q_c. A table where the horizontal value is the angle value divided by 0.1° is then generated, and the value of the vertical coordinates is the hall value on the d- and q-axes.

Table I is generated based on the above description.

The permanent magnet synchronous motor(PMSM) in the open loop system (utilizing the direct-axis current to control the PMSM without the encoder feedback) is controlled,

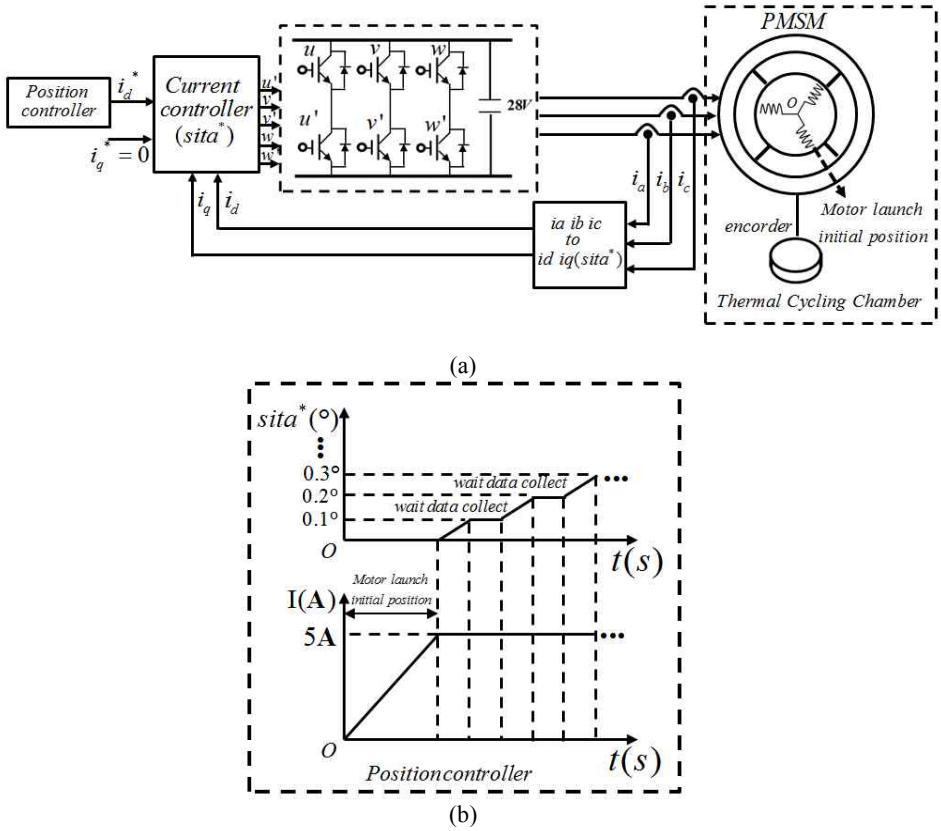

Fig. 7. Positioning process with an open-loop controller. (a) The positioning system structure. (b) The position controller.

which results in accurate positioning of the rotor at 3600 points in the entire round. The PMSM has three stator slots, and the position of each stator slot is fixed, which is unaffected by different temperatures. When the controller outputs the direct-axis current, the rotor will locate at one of the three stator slots shown in Fig. 7(a). The motor then rotates 0.1° each time, and the position controller is shown in Fig. 7(b). The angle used in the position controller is calculated by a micro control unit interrupt timer (Renesas, RX62T, 32-bit floating micro control unit). For example, the interrupt timer is 50 μs, and the rotor rotates by 0.1° in 3 ms. Therefore, the timer adds 2.90888E-05 rad in each control circle (50 μs). The rotor then rotates by 0.1° after 60 times, and the motor speed is 5.555 rpm. Set $i_q^* = 0$, $i_d^* = 5A$, in each positioning process. The temperature in the thermal cycling chamber then changes. The d-q hall values are sampled before and after the temperature changes. The angle value before temperature changes is used to check Table 1 as shown in Fig. 8.

Each sampling point where temperature drift occurs can determine the respective hall values on the d- and q-axes under the initial temperature. Let the initial weight coefficient $\omega_1 = 1$, $\omega_2 = 0$, $\omega_3 = 1$, $\omega_4 = 0$. These coefficients are placed in the error measuring function to complete the first iterative calculation cycle. The steepest descent directions are

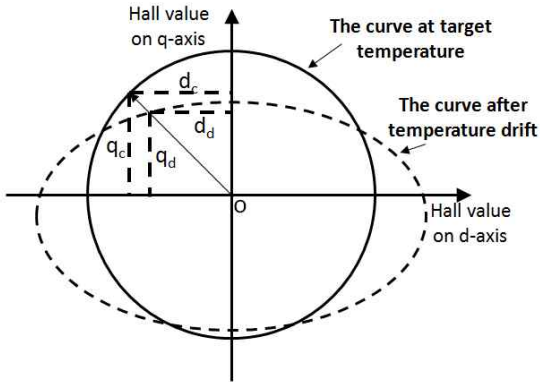

Fig. 8. Diagram of the table look-up process of temperature correction.

used to obtain the four weight coefficients by the gradient method. Formulas (17) to (20) are then used to calculate the weight coefficient value for the next calculation cycle. The new weight coefficient will be used as the correction coefficient in the next calculation. The value of the error measuring function is determined after every calculation cycle finishes. If $V_{i+1}(X) < V_i(X)$, then the calculation continues; otherwise, the calculation is stopped. If $V_i(X) <$ the value set, then the correction coefficient at this point is the most optimal. Fig. 9 shows the whole process of the neuron correction iteration algorithm. Unlike the method in

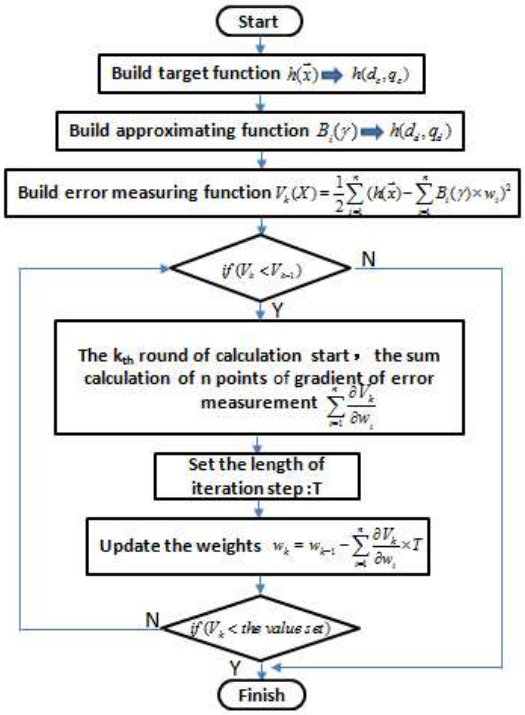

Fig. 9. Flowchart of the neuron iterative calculation algorithm.

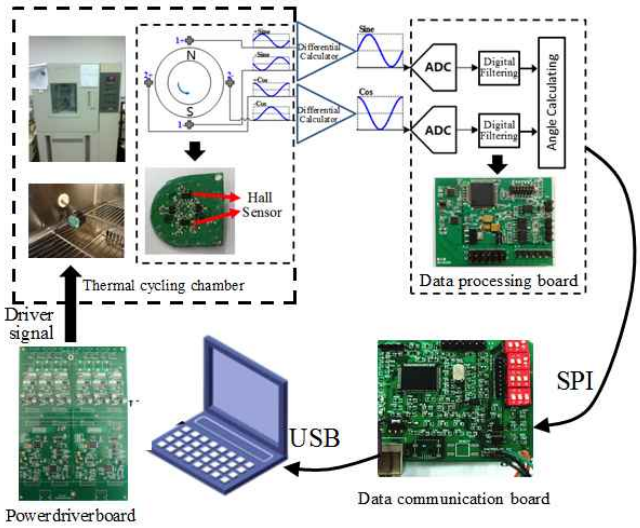

Fig. 10. Configuration of the experimental system.

[7], the proposed method solves the problem without complicated hardware. It can also solve the problem of temperature drift that still exists at high temperature in [6], and the algorithm is simpler than that in [8].

IV. Experimental Results and Analysis

The temperature control cabinet (Fig. 10) is used to change the temperature in this experiment. The angle value of the magneto-electric encoder under +20 °C is set as the target angle value, and its angle value under -40 and +60 °C is the object that has to be modified.

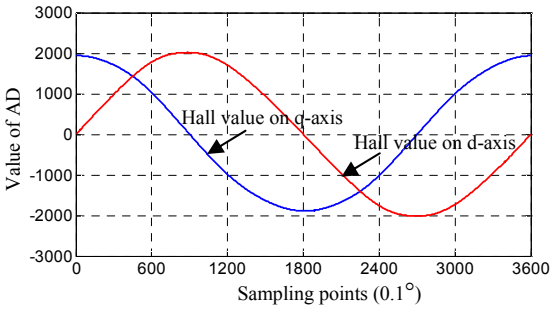

Fig. 11. Hall value of the d- and q-axes under normal temperature.

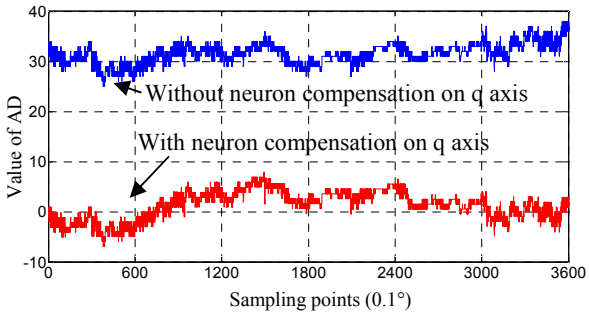

(a)

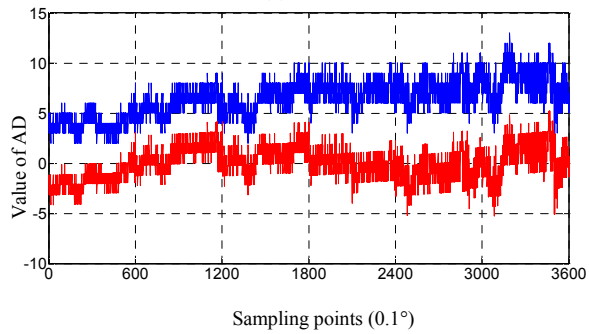

(b)

Fig. 12. Correction effect with the proposed method under temperature changes from +20 °C to -40°C. (a) The deviation value of the hall sensor on the q-axis before and after modification. (b) The deviation value of the hall sensor on the d-axis before and after modification.

Fig. 10 shows that the four hall sensors are used to obtain the hall signals, and the data processing board is utilized to calculate the angle value. The analog signals enter the micro control unit's internal AD module (12-bit Renesas RX62T internal AD), and the sampling period is 50 μs. After signal processing, the SPI communication method is used to transfer the data to the communication board (Renesas 62N which has USB module), which is then used to transfer the data to the computer.

Fig. 11 shows a table based on the angle value under normal temperature and the hall value on the d- and q-axes, and the groups of data are divided by 0.1°. The interpolation calculation for the arbitrary angle is conducted based on this

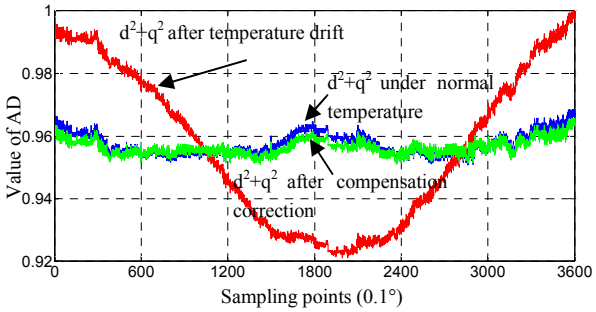

Fig. 13. Value of d^2+q^2 before and after modification under temperature changes from +20 °C to -40 °C.

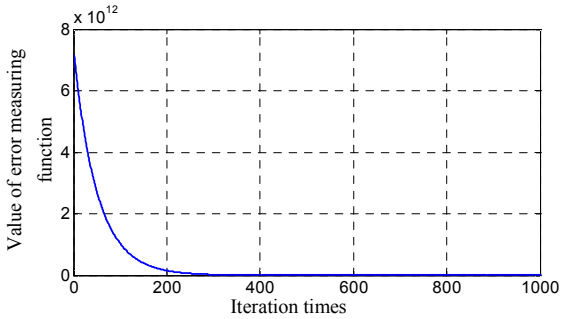

Fig. 14. Convergence curve of the error measuring function.

table to find the hall values on the corresponding d- and q-axes.

Fig. 12(a) shows the difference value between the q-axis hall under target temperature (+20 °C) and q-axis hall after the temperature change (-40 °C) at 3600 positioning points. Fig. 12(b) shows the difference value between the d-axis hall under the target temperature (+20 °C) and d-axis hall after the temperature change (-40 °C) at 3600 positioning points.

The analog signals collected by the four halls are not orthogonally perfect, and the magnetic field-sensitive features of the halls are different. Thus, the hall signals of the d-q axis are not sinusoidally perfect, which makes d^2+q^2 non-constant. This paper mainly discusses the angle compensation after the temperature drift. Fig. 13 shows the value of d^2+q^2 under normal temperature (+20 °C), the value when temperature drift occurs (-40 °C), and the value modified by the neuron compensation algorithm after temperature drift. The value of vertical coordinates divided the maximum value in the collected data, and the horizontal axis means the whole circle is divided by 0.1° into 3600 points.

Fig. 14 shows the convergence curve of the error measuring function when iterated 1000 times with iteration step length T = 0.001. The error measuring function begins to converge to zero after iterating for 200 times.

The PMSM in the open-loop system (utilizing the direct-axis current to control the PMSM without the encoder

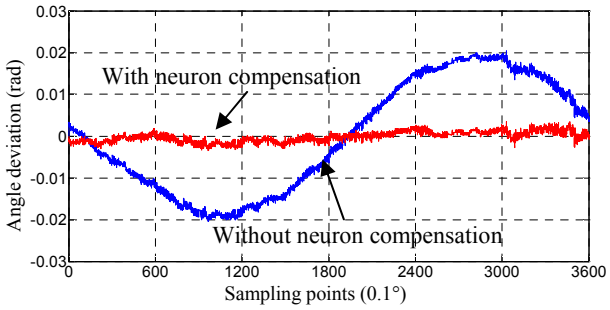

Fig. 15. Deviation of the angle value before and after modification under the temperature change from +20 °C to -40 °C.

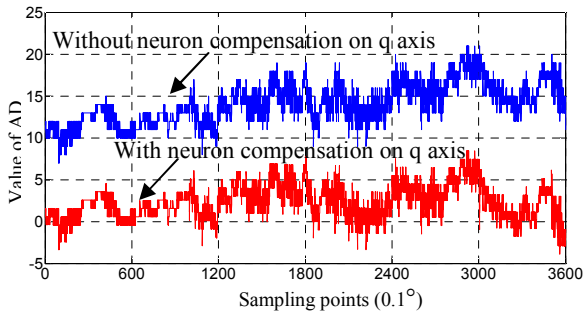

(a)

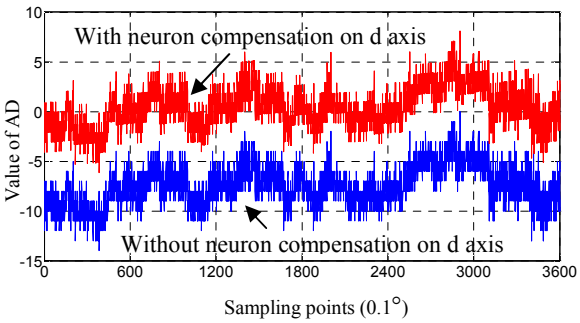

(b)

Fig. 16. Correction effect with the proposed method under the temperature change from +20 °C to +60 °C. (a) The deviation value of the hall sensor on the q-axis before and after modification. (b) The deviation value of the hall sensor on the d-axis before and after modification.

feedback) is controlled, which results in accurate positioning of the rotor at 3600 points in the entire round. The encoder angle is sampled before the temperature changes in the positioning process. The temperature then changes, and then the angle value after the temperature change and that modified with the neuron compensation algorithm are collected. Finally, the experimental results validate that the angle deviation in the proposed method decreases to almost 0, as shown in Fig. 15. The horizontal axis indicates that the whole circle is divided by 0.1° into 3600 points.

Fig. 16(a) shows the difference value between the q-axis hall under the target temperature (+20 °C) and q-axis hall

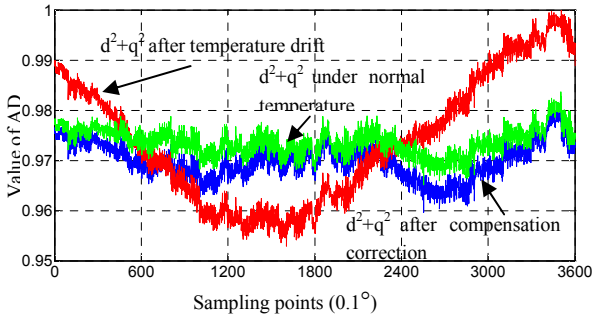

Fig. 17. Value of d^2+q^2 before and after modification under temperature change from +20 °C to +60 °C.

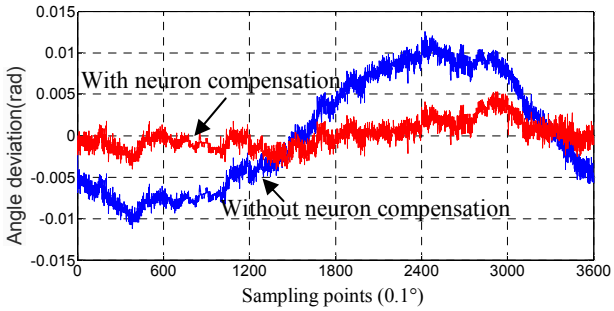

Fig. 18. Deviation of the angle value before and after modification when the temperature changes from +20 °C to +60 °C.

after the temperature change (+60 °C) at 3600 positioning points. Fig. 16(b) shows the difference value between the d-axis hall under the target temperature (+20 °C) and d-axis hall after the temperature change (+60 °C) at 3600 positioning points.

Fig. 17 shows the value of d^2+q^2 under normal temperature (+20 °C), when temperature drift occurred (+60 °C) and the value modified by the neuron compensation algorithm after temperature drift. The vertical coordinate values divide the maximum value in the collected data to facilitate observation.

The angle deviation in the proposed method decreases to almost 0 as shown in Fig. 18 when the temperature changes from +20 °C to +60 °C.

V. CONCLUSIONS

This paper analyzes the cause of angular deflection in magneto-electric encoders when temperature drift occurs as well as proposes a method that uses a temperature compensation algorithm based on neural network. The gradient method is used to initiate fast iterative calculation convergence. The self-adaptive adjustment of the angle value of the magneto-electric encoder is implemented when temperature drift occurs. The effectiveness of the proposed method is verified experimentally. Adaptive correction for angular deflection when the temperature changes from 20 °C to -40 °C and 20 °C to +60 °C is implemented. The angle deviation decreases to almost 0 with the proposed method.

REFERENCES

[1] Z. D. Buckner, M. L.Reed, and J. H.Aylor, "Antialiasing encoder interface with sub-nyquist sampling," *IEEE Trans. Instrum. Meas.*, Vol. 55, No. 6, pp. 2029-2033, Dec. 2006.

[2] C. Attaianese and G. Tomasso, "Position measurement in industrial drives by means of low-cost resolver-to-digital converter," *IEEE Trans. Instrum. Meas.*, Vol. 56, No. 6, pp. 2155-2159, Dec. 2007.

[3] F. T. Jorgensen, T. O. Andersen, and P. O. Rasmussen, "The cycloid permanent magnetic gear," *IEEE Trans. Ind. Appl.*, Vol. 44, No. 6, pp. 1659-1665, Nov./Dec. 2008.

[4] B. Fodor and I. Kollar, "ADC Testing With Verification," *IEEE Trans. Instrum. Meas.*, Vol. 57, No. 12, pp. 2762-2768, Dec. 2008.

[5] A. Flammini, D. Marioli, and E. Sisinni, "A Multichannel DSP-based instrument for displacement measurement using differential variable reluctance transducer," *IEEE Trans. Instrum. Meas.*, Vol. 54, No. 1, pp. 178-183, Feb. 2005.

[6] D. Draxelmayr and R. Borgschulze, "A self-calibrating hall sensor IC with direction detection," *IEEE J. Solid-State Circuits*, Vol. 38, No. 7, pp. 1207-1212, Jul. 2003.

[7] T. Emura, L. Wang, and A. Arakawa, "A high-resolution interpolator for incremental encoders by tow-phase type PLL method," in *Proc. IEEE 19th IECON Conf.,* pp. 1540-1545, 1993.

[8] F. Burger, P.-A. Besse, and R. S. Popovic, "New single chip Hall sensor for three phases brushless motor control," *Sensors and Actuators*, Vol. 81, No. 1, pp. 320-323, Apr. 2000.

[9] B. Ali, D. O. Abdeslam, T. Otmane-Cherif, and H. Seddiki, "Adaptive neural PLL for grid-connected dfig synchronization," *Journal of Power Electronics*, Vol. 14, No. 3, pp. 608-620, May 2014.

[10] R. Kayalvizhi, S. P. Natarajan, and P. Palanisamy, "Development of a neuro controller for a negative output elementary luo converter," *Journal of Power Electronics*, Vol. 7, No. 2, pp. 140-145, Apr. 2007.

[11] Y. Shi, H. Zhang, X. Jiang, Q. Wen, and B. Han, "Design of output voltage waveform on magnetic encoder," *Journal of Magnetism and Magnetic Materials*, Vol. 282, No. SI, pp. 317-320, Nov. 2004.

[12] S. Hao, J. Liu, and Y. Mizugaki, "Development of novel magnetic encoder and vector control method for servo control of high-speed motor," *Journal of Advanced Mechanical Design Systems And Manufacturing*, Vol. 3, No. 4, pp. 345-354, Apr. 2009.

[13] Y. S. Smirnov, T. A. Kozina, E. V. Yurasova, and A. V. Sokolov, "Analog-to-Digital Converters of the Components of a Displacement with the Use of Microelectronic Sine-Cosine Magnetic Encoders," *Measurement Techniques*,Vol. 57, No. 1, pp. 41-46, Apr. 2014.

Lei Wang was born in Harbin, China, in 1986. He received his B.S. in Automatic Control from Harbin University of Commerce, Harbin, China in 2009 and his M.S. in Automatic Control from Harbin Institute of Technology, Harbin, China, in 2011. His current research interests include control theory and its application to motor

systems as well as high-precision magneto-electric encoders.

Shuang-hui Hao was born in Guizhou, China, in 1963. He received his Ph.D. from Kyushu Institute of Technology, Kitakyushu, Japan. He is a professor at the Harbin Institute of Technology, Harbin, China. His current research interests include high precision, high response control technology, and high precision magneto-electric encoders.

Bao-yu Song was born in 1958 in China. He received his B.S. in Mechanical Design in 1982, his M.S. in 1996, and his Ph.D. in 2003 from Harbin Institute of Technology, Harbin, China, where he is a professor. His current research interests include nanometer lubricating material theory and application, new type of sliding bearing technology, and design theory and method of advanced equipment.

Ming-hui Hao was born in Guizhou, China, in 1958. He received his Ph.D. from Kyushu Institute of Technology, Kitakyushu, Japan, in 1994. He is a professor at the Harbin Institute of Technology, Harbin, China. He is the superintendent of the Intelligent Equipment Institute of Technology. His current research interests include CAD/CAM, flexible mechanism of intelligent control technology, and unconventional machining technology.